POLITECNICO DI TORINO
Repository ISTITUZIONALE

# A 20 Mbps, 433 MHz RF ASK Transmitter to Inductively Power a Distributed Network of Miniaturised Neural Implants

*Original*
A 20 Mbps, 433 MHz RF ASK Transmitter to Inductively Power a Distributed Network of Miniaturised Neural Implants / Barbruni, Gian Luca; Asti, Fabio; Ros, Paolo Motto; Ghezzi, Diego; Demarchi, Danilo; Carrara, Sandro. - ELETTRONICO. - (2021), pp. 1-6. (Intervento presentato al convegno 2021 IEEE International Symposium on Medical Measurements and Applications (MeMeA) tenutosi a Lausanne, Switzerland nel 23-25 June 2021) [10.1109/MeMeA52024.2021.9478678].

*Availability:*
This version is available at: 11583/2913905 since: 2021-07-22T09:06:15Z

*Publisher:*
IEEE

*Published*
DOI:10.1109/MeMeA52024.2021.9478678

*Terms of use:*

This article is made available under terms and conditions as specified in the corresponding bibliographic description in the repository

*Publisher copyright*
IEEE postprint/Author's Accepted Manuscript

©2021 IEEE. Personal use of this material is permitted. Permission from IEEE must be obtained for all other uses, in any current or future media, including reprinting/republishing this material for advertising or promotional purposes, creating new collecting works, for resale or lists, or reuse of any copyrighted component of this work in other works.

(Article begins on next page)

01 September 2025

# A 20 Mbps, 433 MHz RF ASK Transmitter to Inductively Power a Distributed Network of Miniaturised Neural Implants


Gian Luca Barbruni
*Medtronic Chair in Neuroengineering and Integrated Circuits Laboratory*
*École polytechnique fédérale de Lausanne*
Switzerland
gianluca.barbruni@epfl.ch

Fabio Asti
*Integrated Circuits Laboratory*
*École polytechnique fédérale de Lausanne*
Neuchâtel, Switzerland
fabio.asti@epfl.ch

Paolo Motto Ros
*DET*
*Politecnico di Torino*
Turin, Italy
paolo.mottoros@polito.it

Diego Ghezzi
*Medtronic Chair in Neuroengineering*
*École polytechnique fédérale de Lausanne*
Geneve, Switzerland
diego.ghezzi@epfl.ch

Danilo Demarchi
*DET*
*Politecnico di Torino*
Turin, Italy
danilo.demarchi@polito.it

Sandro Carrara
*Integrated Circuits Laboratory*
*École polytechnique fédérale de Lausanne*
Neuchâtel, Switzerland
sandro.carrara@epfl.ch



***Abstract*—Simultaneous wireless information and power transfer is an emerging technique in neurotechnology. This work presents an efficient transmitter for both power transfer and downlink data communication to multiple, miniaturised and inductively-powered chips. We designed, implemented and tested a radio-frequency transmitter operating at 433.92 MHz of the industrial, scientific and medical band. A new structure is proposed to efficiently modulate the carrier, exploiting an amplitude-shift keying modulation reaching a data rate as high as 20 Mbps together with a variable modulation index as low as 8%.**



***Index Terms*—Wireless Power Transfer; Inductive Power Transfer; RF Transmitter; ASK Modulator; SWIPT; Implantable Medical Device; Neural Implants; Miniaturisation.**


## I. Introduction

Neurotechnology is a growing research area for treating neurological diseases and mental disorders, which affect a significant fraction of the population. However, most of the Implantable Medical Devices (IMDs) require implantable bulky electronic units and batteries [1], which limit the miniaturisation of the implant. Next-generation neural implants might be composed of a distributed network of miniaturised implants allowing high-density neural stimulation and/or recordings over large areas. In this regard, among the challenges [2], [3], [4], [5], Wireless Power Transfer (WPT) methodologies are key players to control and supply extremely miniaturised and free-floating neural implants [6]. In particular, Simultaneous Wireless Information and Power Transfer (SWIPT) systems have been widely investigated. The power required by such miniaturised implants depend on the application (i.e. recording, surface stimulation, deep brain stimulation). Fig. 1a depicts the case of multiple miniaturised brain implant (i.e. sub-mm size), wirelessly powered via 3-coils inductive link and designed for brain stimulation. In this case, 20-100 µW are usually required for the operation of the entire chip. Fig. 1b shows a simplified equivalent scheme of the entire path:


This work was supported by the Interdisciplinary Seed Fund from École polytechnique fédérale de Lausanne.


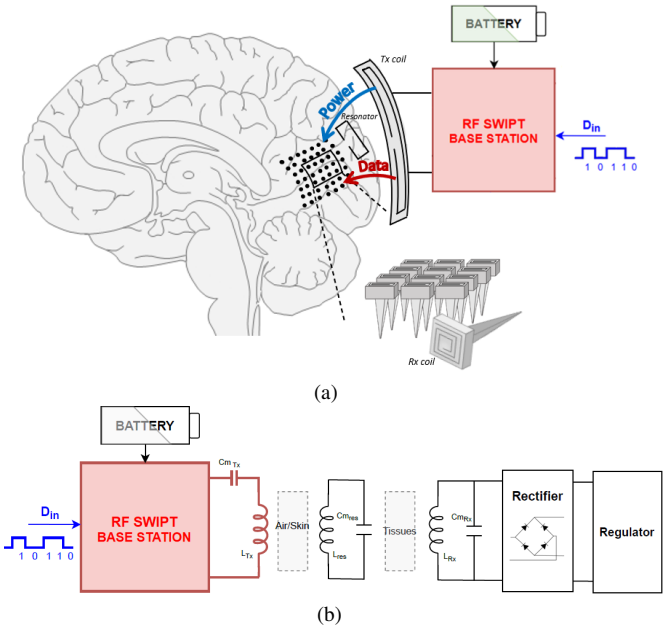


Fig. 1: (a) 3-coils IPT link in a distributed network of ultra-miniaturised neural implants. (b) General equivalent scheme for a 3-coils IPT link. In red, the novel RF SWIPT transmitter proposed in this paper.

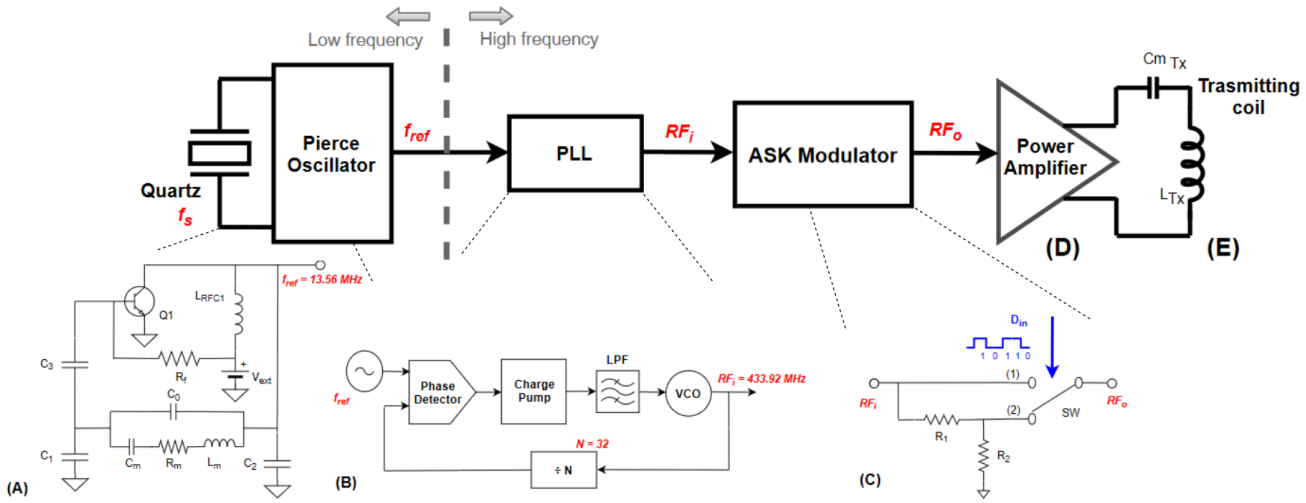


Fig. 2: Main blocks of the external RF transmitter: (A) LF Pierce oscillator; (B) PLL; (C) ASK modulator; (D) PA; (E) Transmitting coil (Tx).

from the common Radio-Frequency (RF) base station front-end (highlighted in red and scope of this paper) to the single, individual neural implant back-end.

## II. System Concept

Several WPT systems have been proposed over the last years for miniaturised implants, including: magnetic coupling, electromagnetic radiation, visible or near-infrared radiation and ultrasonic coupling. Among WPT methods, 3-coils Inductive Power Transfer (IPT) emerged as the most appropriate method to supply multiple miniaturised chips with a medium penetration depth (i.e. 1-2 cm) [7]. WPT via IPT to miniaturised receiving coil (Rx) is mainly limited by low Rx quality factor $Q$, low magnetic coupling at high distances and Specific Absorption Rate (SAR). 3-coils IPT systems showed the best performance in terms of Power Transfer Efficiency (PTE), tolerance to misalignment and SAR-constrained Power Delivered to the Load (PDL) [8]. Also, the efficiency of the driver is negligible for 3-coils systems. PTE and PDL are two key parameters in IPT links. High PTE favours the reduction of heat dissipation within the coils and the tissue exposure to the magnetic field $\mathcal{H}$. IPT with multiple coils showed PTE increments even at large operating distance compared to 2-coils IPT systems [8]. In the case of miniaturised wirelessly powered IMDs, the large majority of design constrains come from the implant side and, therefore, the efficiency of the Tx side may be sacrificed for a more robust and insensitive base station. Moreover, in distributed network of miniaturised implants, each powering transmission line (from the common Tx front-end to the single receiver back-end) has a different impedance. As a consequence, the Power Amplifier (PA) of the RF SWIPT system needs to be a trade-off between power, gain, linearity and robustness.

Data transfer is another key element in the design of RF SWIPT transmitters [9] for several distributed and extremely miniaturised implants requiring large data transmission (e.g. up to a few tens of Mbps) [10]. Data communication needs to be robust enough against interference to keep an optimal bandwidth. Several modulation techniques for RF data transmission have been proposed over the last years. Among the other, Amplitude-Shift Keying (ASK), On-Off Keying (OOK), Frequency-Shift Keying (FSK), Phase-Shift Keying (PSK) and Pulse Position Modulation (PPM). ASK modulation is usually used for its circuital simplicity, low area and power consumption (considerations also valid for the implant side's demodulation block). The key parameter in ASK modulation is the Modulation Index (MI), which considers the amplitude difference between "high" and "low" logical states [11]. In particular, no modulation occurs for $MI = 0$ and OOK modulation is performed for $MI = 1$. In the case of miniaturised implant, the energy storing elements are extremely minimised, being the SWIPT signal the only source of energy. As a consequence, if the signal is turned off, the chip is no more supplied. Therefore, a sophisticated OOK communication protocol needs to be adopted, controlling the maximum number of subsequent "low" logical transmitted bits to maintain the transistor in their normal working condition. Both FSK [12] and PSK modulation [13] are less susceptible to noise with respect to ASK, at the cost of more complex circuital systems and a low achievable data rate [14]. They exhibit a larger frequency bandwidth, which is critical with high-$Q$ coils [9]. Moreover, in 3-coils IPT systems, the high-$Q$ resonator inhibits frequency and phase variations of the transferred signal [15]. PPM presents a good synchronisation and simplify the clock recovering at the implant side. An exciting implementation is the Pulse-Width Modulated-ASK (PWM-ASK) [6], which shows improvement in Bit Error Rate (BER) and signal to noise ratio. On the contrary, both PPM and PWM-ASK suffer from a low data rate. The optimal modulation technique is a trade-off between carrier frequency, data rate, sensitivity, circuital complexity, distance, area and power consumption for both the transmitting and receiving

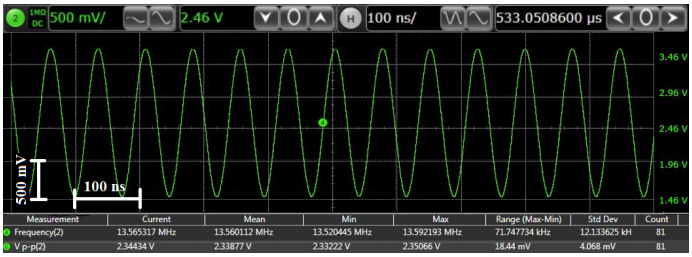


Fig. 3: Measurement of 13.56 MHz Pierce oscillator.

side [9]. In general, data rate may be increased by increasing the carrier frequency $f_0$. However, the maximum $f_0$ is limited to a few hundreds of MHz due to dielectric power losses in biological tissues, exponentially increasing with the frequency. Moreover, SAR is proportional to $f_0$, hence, decreasing $f_0$ is beneficial to increase the transmitted power and, finally, to maximise the PDL. At the same time, a low $f_0$ implies a large matching capacitor at the receiver side, which increases the bulkiness of the implant. Therefore, $f_0$ is selected as a trade-off between size constrains (which becomes significant at low frequencies) and PTE (which decreases with the frequency). As a rule of thumb, the optimal $f_0$ must be higher than 250 MHz to enable Rx miniaturisation, and lower than 2.5 GHz to reduce tissue losses and to have sufficient PTE [16]. Moving from cm to mm-sizes, the optimal $f_0$ consequently increases from a few MHz to hundreds of MHz. We selected 433.92 MHz of the Industrial, Scientific and Medical (ISM) radio band as optimal $f_0$ for the IPT system, which is a good trade-off between miniaturisation (i.e. under mm-range) and good PTE and SAR-constrained PDL [17]. Here, we propose a novel RF transmitter exploiting ASK modulation with a high data rate together with an ultra-low MI.

## III. System Design and Architecture

Fig. 2 shows the RF transmitter architecture. It is composed by a quartz, a Low Frequency (LF) Pierce oscillator, a Phase-Locked Loop (PLL), an ASK modulator, a class-AB PA and a transmitting coil (Tx).

### A. Low Frequency Pierce Oscillator

The first electronic block is the reference oscillator in Pierce configuration (Fig. 2-A). In general, crystal-based Pierce configuration is used with quartz oscillating in the range 9.735 ÷ 14.0625 MHz, being advantageous in terms of cost, size and power consumption. Fig. 2-A also shows the lumped model of the quartz crystal described with the motional resistance $R_m$, the motional capacitance $C_m$, the motional inductance $L_m$ and the package capacitance $C_0$. The resonating frequency $f_{ref}$ of the quartz crystal is 13.56 MHz, as in Fig. 3; and the lumped elements are determined accordingly (i.e. $R_m = 60\ \Omega$, $C_m = 0.012003\ pF$, $L_m = 11.477\ mH$ and $C_0 = 2.949\ pF$). The Pierce oscillator's parameters showed in Fig. 2-A (e.g. $R_f$, $C_1$, $C_2$, $C_3$, $L_{RFC1}$) have been sized following the design procedure described in [18]. In particular, the feedback resistance $R_f$ is inversely proportional to the frequency and

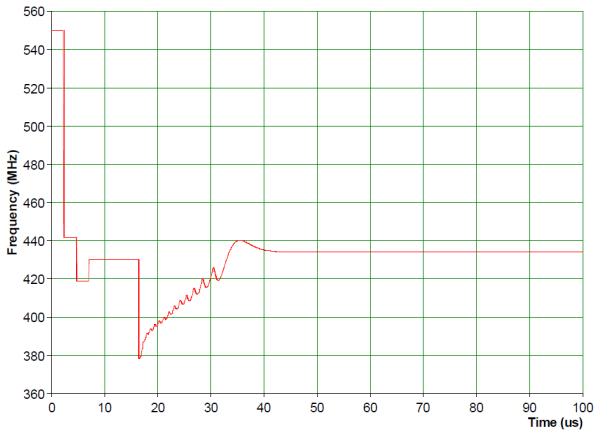


(a)

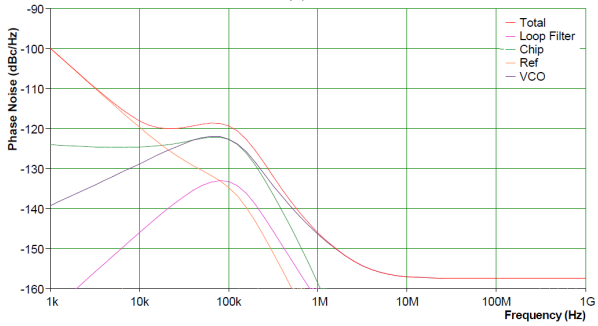


(b)

Fig. 4: Simulations of (a) PLL $RF_i$: the calibration time before reaching the stable $RF_i$ depends on the B-divider value (i.e. 16); and (b) Phase noise behaviour highlighting the contributes of the "VCO" - voltage controlled oscillator; "Ref" – internal reference oscillator (i.e. 550 MHz); "Loop Filter" and "Chip" - noise of the loop filter, dividers and phase detector components modulating the VCO respectively.

it has been chosen equal to 1 MΩ, thus preventing physically damages of the crystal [19]. Assuming a lossless oscillator, $f_{ref}$ is given as in (1):

$$f_{ref} = f_s \cdot (1 + \rho_c) = \frac{1}{2\pi\sqrt{L_m\, C_m}} \cdot \left(1 + \frac{C_m}{2\, C_L}\right) \qquad (1)$$

where $f_s$ is the series resonant frequency of the crystal, $\rho_c$ is the pulling factor and $C_L$ is the load capacitance (i.e. 20 $pF$, [20]). Hence, $C_L$ is described as in (2):

$$C_L = \frac{C_1\, C_2}{C_1 + C_2} + PCB_{strays} \qquad (2)$$

where $PCB_{strays}$ is the stray capacitance of the printed circuit board (i.e. 3 $pF$). In general, the transistor $Q_1$ (i.e. a BJT in *npn* configuration) have a small parasitic capacitances and they have been neglected in (2). Therefore, solving (2) and supposing equal capacitance values, $C_1$ = $C_2$ = 27 $pF$ [20]. Last, $L_{RFC1}$ represents the inductor choke, used to provide a constant current from the power supply $V_{DD}$ provided from an external battery (i.e. $L_{RFC1} = 4.7\ mH$ for a $V_{DD} = 3.6\ V$).

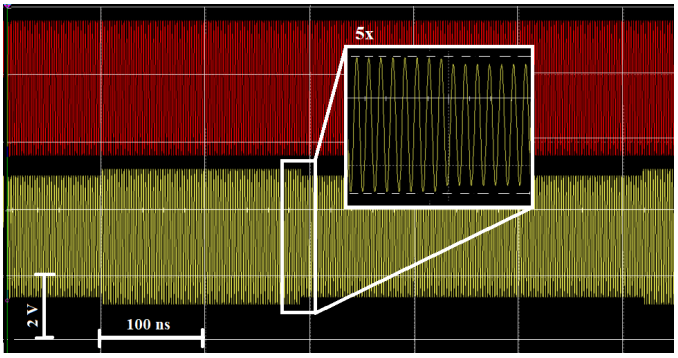


Fig. 5: Simulation of our new ASK modulation approach. Red and yellow sine waves are $RF_i$ and $RF_o$ respectively. The zoom highlights the ASK with a MI of 8%.

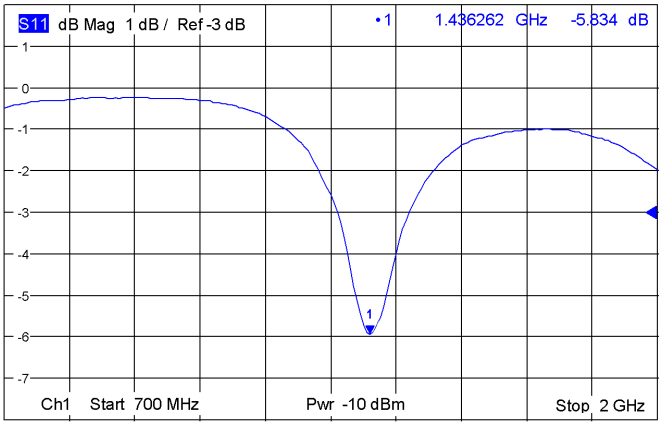


Fig. 6: Measurement of Tx return loss $S_{11}$ (in dB).

### B. Phased-Locked Loop

PLL is used in a wide variety of high-frequency applications, mainly in radio communication at high performances and in transceivers, providing a precise and stable output frequency $RF_i$ starting with an input reference frequency $f_{ref}$ [21]. We selected an integer-N PLL with $N = 32$, calculated as the ratio between $RF_i$ (i.e. 433.92 MHz) and $f_{ref}$ (i.e. 13.56 MHz). The choice of the integer-N PLL (LTC6948-1 by Analog Devices) is a trade-off between several parameters (e.g. reference frequency, operating frequency range, phase noise and frequency spur limitations), as in [22]. As a rule of thumb, the PLL input impedance needs to be matched to minimize reflections. Therefore, the input parallel capacitance should be small enough to avoid input noise that can arise in the loop. As a result, PLL locks the $RF_i$ of 433.92 MHz after 45 $\mu$s (Fig. 4a). The PLL phase noise is simulated around to -158 dBc/Hz at $RF_i$, as in Fig. 4b.

### C. ASK Modulator

ASK modulation minimises bulkiness and power dissipation both in the transmitting and receiving side. One of the most important parameter in ASK modulation is the MI, defined as in (3):

$$MI = \frac{V_{max} - V_{min}}{V_{max} + V_{min}} \tag{3}$$

where $V_{max}$ and $V_{min}$ are respectively the peak amplitude of the voltages for the logical "high" and "low" states. Indirectly, MI influences the BER and, therefore, its reliability. On the one side, high MI means a big difference between the two voltages $V_{max} - V_{min}$ and, therefore, low BER, since detection between logical "high" and "low" states is simplified. On the other side, high MI means high power consumption on the demodulation side, which is the most critical part of the whole system design. As a consequence, even if a low MI ASK transmitter is very challenging, it results to be the best candidate for this application. Our approach is based on a switch and a symmetrical T-pad voltage attenuator, as shown in Fig. 2-C. More in detail, the circuit works as in (4):

$$RF_o = \begin{cases} RF_i & if\ SW = 1 \\ RF_i \cdot \frac{R_2 \| R_3}{R_1 + R_2 \| R_3} = RF_i \cdot (1 - MI) & if\ SW = 2 \end{cases} \tag{4}$$

where $RF_o$ and $RF_i$ are respectively the signals before and after the modulation block, $R_1$, $R_2$ and $R_3$ are the three resistances of the T-pad attenuator. In particular, $R_2$ may be modified to obtain a system with a variable MI (i.e. for $MI = 0.08$, $R_1 = R_3 = 10\ \Omega$, $R_2 = 470\ \Omega$, as in Fig. 5). The switch is characterized by an internal driver designed for wide-band applications (M3SW-2-50DRA+ by Mini-Circuits'). Accordingly with a data rate as high as 20 Mbps, the switching times need to be smaller than 50 ns (i.e. our switch has rising time $t_{rise} = 3.3\ ns$ and falling time $t_{fall} = 4.6\ ns$).

### D. Power Amplifier

The PA is necessary to enforce the robustness of the RF SWIPT, also facing issues related to interference, power consumption and gain. The class-E PA is generally selected for power signals due to several advantages: simple design, high power transmission, low power consumption and the highest efficiency [26]. On the other side, it is susceptible on the effects of adjusting load-network components: a slight network variation causes a significant variation in the powering signal. This condition finally leads to a sensitive Tx system which may cause losses in robustness. In particular, we used a class-AB PA (RF5110G by Qorvo) characterised for RF applications in the 150-960 MHz frequency range and internally matched at 50 $\Omega$. At 433.92 MHz, 32 dBm can be transmitted, with a very high PA gain of 41 dB at the cost of reduced efficiency of 38%.

### E. Transmitting coil Tx

In the case of 3-coils IPT systems for multiple miniaturised implants, the resonator diameter $d_{Res}$ is selected from the area of coverage, which is always application-constrained. Then,

TABLE I: STATE-OF-THE-ART COMPARISON OF RF SWIPT TRANSMITTER ON IPT LINK.

| Year, Ref | Carrier Frequency (MHz) | Modulation Technique (Downlink) | Data Rate (Mbps) | Output Power (dBm) | Efficiency (%) | Voltage source (V) | FOM (Mbps$^2$/ MHz)$^{1/3}$ |
|---|---|---|---|---|---|---|---|
| 2020, [6] | 915 | PWM-ASK | 1 | 8 | NA | 0.6 ÷ 1 | 0.11 |
| 1997, [23] | 10 | ASK | 0.12 | NA | 99* | 5 | 0.12 |
| 2013, [12] | 915 | FSK | 1.5 | 0 | 18 | 1.2 | 0.14 |
| 2004, [11] | 0.7 | ASK | 0.06 | 17 | 36 | 5 | 0.18 |
| 2018, [24] | 10 | ASK | 1 | 13.8 | 42 | 2.4 | 0.46 |
| 2008, [25] | 433 | OOK | 10 | -12.7 | 4.5 | 1 | 0.62 |
| **This work** | **433** | **ASK** | **20** | **32** | **38*** | **5** | **0.97** |

* PA only

the optimal Tx diameter $d_{Tx}$ that will maximise the magnetic coupling with the resonator is calculated as [27]:

$$d_{Tx} = \sqrt{{d_{Res}}^2 + 4 \cdot {d_{12}}^2} \tag{5}$$

where $d_{12}$ is the Tx-resonator distance. In particular, $d_{Tx} \simeq 40\ mm$ for a $d_{Res} = 10\ mm$ and a $d_{12} = 20\ mm$, reasonable values for thousands of sub-mm neural implants. Operating at 433.92 MHz, the number of Tx turns is mainly limited by the Self Resonance Frequency (SRF). A single turn Tx coil is selected to limit the SRF degradation. As a result, the return loss $S_{11}$ measurement of our squared Tx coil is shown in Fig. 6.

## IV. Results and Discussion

Fig. 7 shows the testbench with the final result of the study. The measured output of the PA highlights the ASK modulation performed with a MI of 8%. 14.8 and 14.4 dBm are respectively measured for the "high" and "low" states of the SWIPT system for an $RF_i$ of -30 dBm. The transition times present some glitches due to the high rising and falling times of the digital waveform generator (which are comparable with the switching times of our ASK modulator). Table I compares the RF transmitter with the state-of-the-art, highlighting some relevant parameters in SWIPT systems. The relation between data rate and carrier frequency is fundamental in evaluating the performance of SWIPT systems. In particular, we propose a new Figure of Merit (FoM), measured in (Mbps$^2$/MHz)$^{1/3}$ and defined as:

$$FOM = \sqrt[3]{\frac{DR^2}{f_0}} \tag{6}$$

where DR is the data rate (in Mbps) and $f_0$ is the carrier frequency (in MHz). As a rule of thumb, DR may be increased by increasing $f_0$ while obtaining a high FoM is increasingly challenging as $f_0$ increases. Therefore in (6), $DR^2$ is used instead of $DR$. The cubic root further highlights significant changes in FoM values between the different RF transmitters of Table I. On the one side, OOK architectures present high FoM due to simple modulation and demodulation scheme. On the other side, in miniaturised chips, OOK modulation is

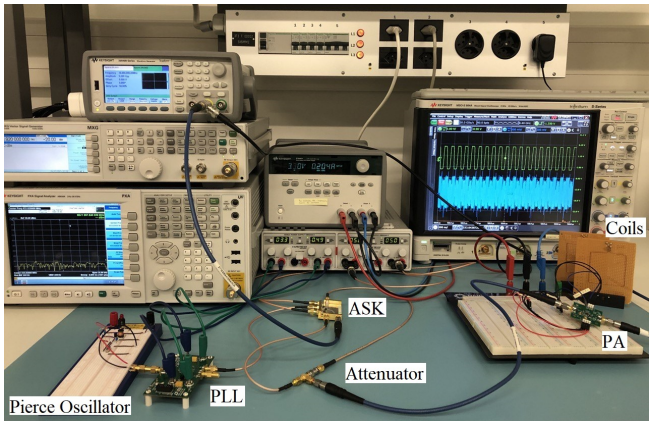


(a)

(b)

Fig. 7: Testbench (a) and measurements (b) of our RF ASK transmitter. The system efficiently modulate a square wave with a duty cycle of 50% at 20 Mbps.

critical in providing a stable supply at the implant side. As expected, FSK transmitters show low values of FoM since they cannot provide high DR. Finally, basing on the new FoM, our SWIPT transmitter shows better performance with respect to similar work previously published. Then, most of the SWIPT systems use a class-E PA, which usually ensures efficiencies higher than 97%. Moreover, the RF modulation

is usually performed operating directly on the class-E PA circuitry. As an example, Navaii and collaborators proposed a Darlington emitter-follower, which changes the supply voltage of a class-E PA, which is connected to the transistor's drain, performing the amplitude modulation, guarantying an optimal PTE [24]. However, this approach results to be very sensitive to the inductive parameters of the transmission (e.g. Tx and Rx inductances, matching networks, penetration depth), being critical in SWIPT systems with very high data rate. Instead, we decided to use a class-AB PA, leading with a higher output power (the highest of Table I), an improved robustness against impedance variations at the cost of a reduced efficiency. Moreover, differently from [24], we perform the RF ASK modulation before the amplification stage (as in Fig. 2). As a result, we obtain a data rate of 20 Mbps, which is the highest with respect to other similar SWIPT systems.

## V. Conclusions

Over the last years, wireless power transfer has shown tremendous advantages for next-generation implantable neural systems. Miniaturisation and large scale distribution are crucial elements for the future of precise medicine and therapy. In particular, wireless power transfer via inductive links has shown promising results in efficiency and robustness. In this paper, a novel RF structure is designed and measured for simultaneous wireless power transfer and downlink data communication. The strengths and weaknesses of the present state-of-the-art have been analysed. The results highlight the feasibility to transmit a carrier signal at 433.92 MHz, combining power transfer with a novel ASK modulation structure. Each block of the whole chain has been simulated, implemented and tested starting from some off-the-shelf components. This study shows a RF transmitter, amplitude modulated with a data rate as high as 20 Mbps and a variable modulation index as low as 8%. Future work will include PCB fabrication of the whole system, including the printed transmitting coil. The final transmitter will be used to characterise and test the 3-coils inductive link itself with miniaturised receivers. At the very end, high data rate and low modulation index might enable the implantation of thousands of freestanding and miniaturised neural implants.

## Acknowledgment

This work was supported by the Interdisciplinary Seed Fund from École polytechnique fédérale de Lausanne.

## References

[1] P. Gutruf et al. "Fully implantable optoelectronic systems for battery-free, multi modal operation in neuroscience research". In: Nature Electronics 1.12 (2018), pp. 652–660.

[2] S. Carrara, "Body Dust: Well Beyond Wearable and Implantable Sensors," in IEEE Sensors Journal (2020).

[3] G. L. Barbruni, P. M. Ros, S. Aiassa, D. Demarchi and S. Carrara, "Body Dust: Ultra-Low Power OOK Modulation Circuit for Wireless Data Transmission in Drinkable sub-100μm-sized Biochips". arXiv preprint arXiv:1912.02670 (2019).

[4] P. M. Ros, B. Miccoli, A. Sanginario and D. Demarchi, "Low-power architecture for integrated CMOS bio-sensing," 2017 IEEE Biomedical Circuits and Systems Conference (BioCAS), Turin, Italy, 2017, pp. 1-4.

[5] P. M. Ros, A. Sanginario, M. Crepaldi and D. Demarchi, "Quality-Energy Trade-off and Bio-Inspired Electronic Systems," 2018 IEEE International Conference on the Science of Electrical Engineering in Israel (ICSEE), Eilat, Israel, 2018, pp. 1-5

[6] J. Lee et al. "Wireless ensembles of sub-mm microimplants communicating as a network near 1 GHz in a neural application". In: bioRxiv (2020).

[7] G. L. Barbruni et al. "Miniaturised wireless power transfer systems for neurostimulation: a review". In: IEEE Transactions on Biomedical Circuits and Systems 14.6 (2020), pp. 1160–1178.

[8] M. Kiani, U. M. Jow, and M. Ghovanloo. "Design and optimization of a 3-coil inductive link for efficient wireless power transmission". In: IEEE transactions on biomedical circuits and systems 5.6 (2011), pp. 579–591.

[9] B. Lee and M. Ghovanloo. "An overview of data telemetry in inductively powered implantable biomedical devices". In: IEEE Communications Magazine 57.2 (2019), pp. 74–80.

[10] M. Monge et al. "A fully intraocular high-density self-calibrating epiretinal prosthesis". In: IEEE Transactions on Biomedical Circuits and Systems 7.6 (2013), pp. 747–76.

[11] M. Catrysse, B. Hermans, and R. Puers. "An inductive power system with integrated bi-directional data transmission". In: Sensors and Actuators A: Physical 115.2-3 (2004), pp. 221–229.

[12] K. Abdelhalim et al. "915-MHz FSK/OOK wireless neural recording SoC with 64 mixed-signal FIR filters". In: IEEE Journal of Solid-State Circuits 48.10 (2013), pp. 2478–2493.

[13] Y. Hu and M. Sawan. "A fully integrated low-power BPSK demodulator for implantable medical devices". In: IEEE Transactions on Circuits and Systems I: 52.12 (2005), pp. 2552–2562.

[14] F. Beach. "Electrical systems and equipment". In: Third Edition. British Electricity International. Oxford: Pergamon, 1992. Chap. 8, pp. 649–747.

[15] S. A. Mirbozorgi et al. "A single-chip full-duplex high speed transceiver for multi-site stimulating and recording neural implants". In: IEEE Transactions on Biomedical Circuits and Systems 10.3 (2015), pp. 643–653.

[16] A. S. Poon, S. O'Driscoll, and T. H. Meng. "Optimal operating frequency in wireless power transmission for implantable devices". In: 2007 29th Annual International Conference of the IEEE Engineering in Medicine and Biology Society. IEEE. 2007, pp. 5673–5678.

[17] N. Ahmadi et al. "Towards a distributed, chronically-implantable neural interface". In: 2019 9th International IEEE/EMBS Conference on Neural Engineering (NER). IEEE.2019, pp. 719–724.

[18] K. K. Lee, K. Granhaug, and N. Andersen. "A study of low-power crystal oscillator design". In: 2013 NORCHIP. IEEE. 2013, pp. 1–4.

[19] R. Cerda. "Pierce-gate crystal oscillator, an introduction". In: Crytek Corporation (2008), p. 1.

[20] S. Raza. "Fundamentals: understanding the basics of the Pierce oscillator". 53 (July 2011).

[21] B. Razavi. RF microelectronics. Vol. 2. Prentice Hall New York, 2012.

[22] R. Sun. "How to design and debug a phase-locked loop (PLL) circuit". In: Analog Dialogue 47 (2013).

[23] J. Parramon et al. "ASIC-based batteryless implantable telemetry microsystem for recording purposes". In: Proceedings of the 19th Annual International Conference of the IEEE Engineering in Medicine and Biology Society. Vol. 5. IEEE. 1997, pp. 2225–2228.

[24] M. L. Navaii, H. Sadjedi, and A. Sarrafzadeh. "Efficient ASK data and power transmission by the class-E with a switchable tuned network". In: IEEE Transactions on Circuits and Systems I: Regular Papers 65.10 (2018), pp. 3255–3266.

[25] M. K. Raja and Y. Ping Xu. "A 52 pJ/bit OOK transmitter with adaptable data rate". In: 2008 IEEE Asian Solid-State Circuits Conference. IEEE. 2008, pp. 341–344.

[26] S. M. Abbas, M. A. Hannan, and A. S. Salina. "Efficient class-E design for inductive powering wireless biotelemetry applications". In: 2012 International Conference on Biomedical Engineering (ICoBE). IEEE. 2012, pp. 445–449.

[27] U. Jow and M. Ghovanloo. "Optimization of a multiband wireless link for neuroprosthetic implantable devices". In: 2008 IEEE Biomedical Circuits and Systems Conference. IEEE. 2008, pp. 97–100.